Detonation and High-Speed Imaging of PETN Energetic Materials

Atharva Gujrathi*, Andy Zheng†

Understanding the ignition and detonation process of energetic materials is pivotal in improving their safety and performance. Key to conducting detonation experiments is a method of both safely and reliably detonating the energetic material of interest. The primary focus of this work is the design of novel sample mounts that hold energetic materials for detonation experiments. Experiments are conducted using these sample mounts with varying amounts and forms of pentaerythritol tetranitrate (PETN), including powder form and crystal form. These detonations are recorded with a Shimadzu Hyper Vision HPV-X2 high-speed camera, which allows for observation of the ignition process, the propagation of the detonation wave, and qualitative energy release. Results show that the slot design for sample mounts detonate reliably and provide an acceptable working geometry for imaging detonations. Finally, with the slot sample geometry, it was seen that the detonation speed is dependent on the amount of PETN used and the packing density.

I. Nomenclature

H = slot height (mm)
L = slot length (mm)
W = slot width (mm)

II. Introduction and Motivation

Energetic materials are important to characterize in many fields of aerospace engineering. This includes explosives in stage separation of rockets, igniters for recovery deployment, and initiators. Although energetic materials are widespread in use, their behavior is not very well understood. Characterizing the ignition sequence and detonation process will allow for improvements in both performance and safety.

This research conducted in the Sensing Technologies Lab under the George W. Woodruff School of Mechanical Engineering involved the detonation and analysis of pentaerythritol tetranitrate (PETN) samples in varying forms and masses. PETN is a secondary explosive, which means it requires a large amount of energy in order to detonate. This energy can come from various sources, including detonators, electron beams [1], and thermal ignition [2]. PETN comes in two main forms: a white crystalline powder form with texture similar to sand, and a single crystal, which comes from mixing PETN with a solvent and evaporating the solvent, leaving behind a precipitate [3]. These forms, along with the PETN atomic structure, are shown in Fig. 1.

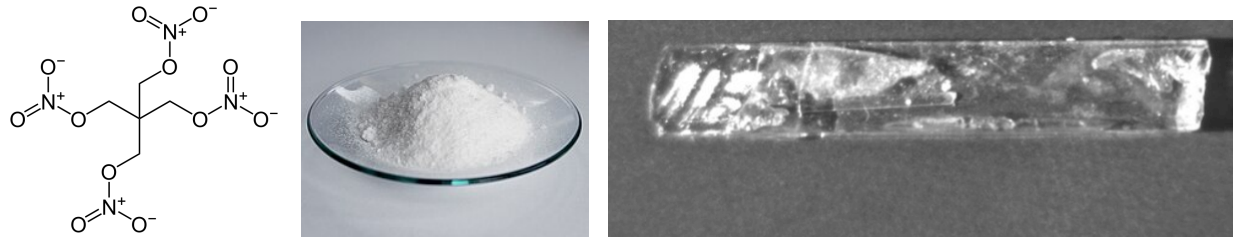

(a) **(b)** **(c)**

Fig. 1 a) PETN crystal structure, b) PETN in powder form, and c) a single crystal of PETN are shown.

*Undergraduate Member, Sensing Technologies Lab, Daniel Guggenheim School of Aerospace Engineering, AIAA Student Member 1603265
†Graduate Advisor, Sensing Technologies Lab, George W. Woodruff School of Mechanical Engineering, AIAA Member 1218751

Experiments were run with a single detonation of samples of PETN powder or crystals. These samples were placed in a novel sample mount design, which were then detonated using a gold bridge-wire detonator. The detonation event was recorded with a Shimadzu HPV-X2 camera recording at a rate of 10 million frames per second (FPS). In order to conduct these detonations safely, a large-scale, modular "detonation box" was developed prior to these experiments which provided the necessary optics and containment method for imaging the samples. This report details the design and manufacturing of the detonation box and sample mounts, along with detonation results and analysis.

III. Experimental Setup

A. Detonation Box

Previous experiments used an existing smaller-scale prototype box constructed using 80/20 T-slot aluminum bars for the frame and polycarbonate sheets for the walls. This version featured a borosilicate glass window for high-clarity imaging. Although functional, the design revealed several limitations, including structural weaknesses and insufficient attachment points for wiring of the detonator to the firing set. Figure 2a depicts the older prototype.

To address these problems, a larger, more robust design for the detonation box was proposed. The updated model retained the T-slot frame and polycarbonate walls but introduced additional structural reinforcements and features. Improvements included an electrical port for detonator connections and an upgraded window frame design. The borosilicate glass windows were thickened to withstand higher pressures, and 3D-printed materials were utilized for durability and replacement. Material and structural calculations were conducted to ensure the enclosure could withstand the energy released by 200 mg of PETN, which equates to 1.162 kJ. The reflected pressure caused by this PETN explosion was calculated to be 639.81 kPa. Polycarbonate sheets with a compressive yield strength of 18 MPa and an Izod impact strength of 10 kJ/m^2 were deemed suitable for the application, as it had a significant Factor of Safety (FoS) for the tested PETN amounts. Figure 2 shows the different components of the detonation box.

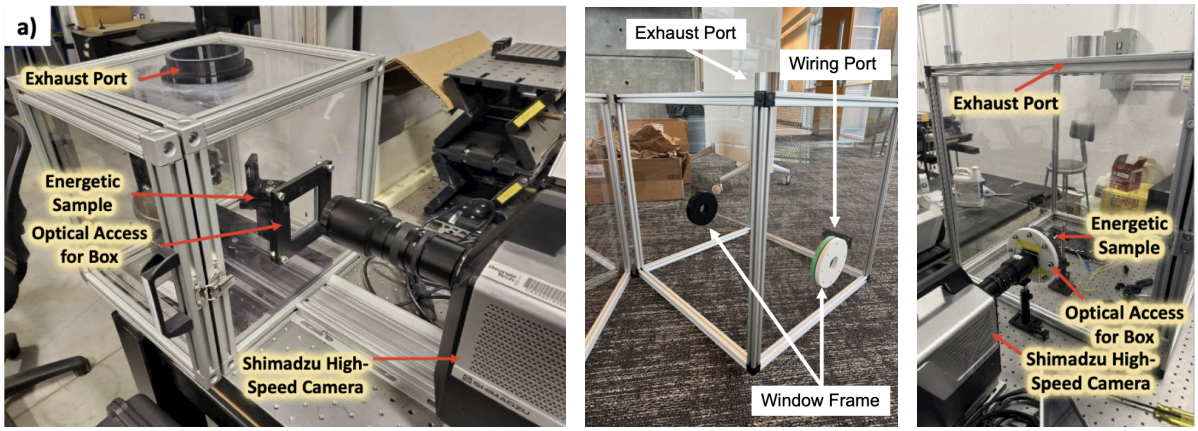

(a) **(b)** **(c)**

Fig. 2 a) The prototype box, b) the detonation box during manufacturing, and c) the box in testing are shown.

Minor issues found in initial rounds of testing included window shattering and risk of arcing in the electrical connections. Along with fixing the aforementioned issues, subsequent modifications included installing rubber padding to the door frame, reinforcing the wiring port, and upgrading window mounts. These adjustments significantly improved the durability of the box during testing. Figure 3 highlights the improvement to the window design and the current window configuration.

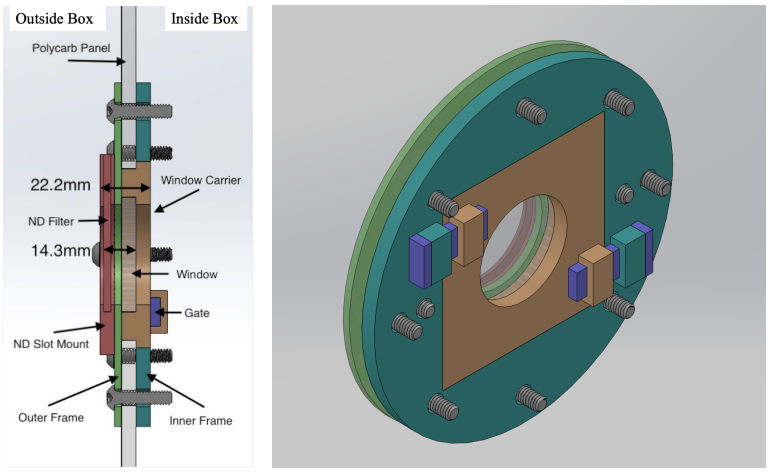

(a) **(b)**

Fig. 3 Detonation box window frame and a cross-sectional view of the updated window mount is shown.

B. Sample Mounts

The novel design of the sample mounts involved a slot design to place samples of varying mass and packing density. Packing density is defined by the amount of mass of powdered PETN in a particular volume in relation to the Theoretical Maximum Density (TMD), which is 1.77 g/cm^3 [4]. Because of the granular form of PETN powder, which in these experiments were measured to be 0.2 to 0.4 μm in diameter, the packing density achievable is only a percentage of the TMD. This percent-TMD is a key parameter explored in the sample mount design. The feasibility of PETN crystals to detonate was also taken into consideration. Due to the crystal structure [5], crystals are more sensitive to detonation along the *c*-axis. This is because the intermolecular forces between crystal layers in the *c*-axis are dominated by Van der Waals forces, whereas the molecules in the *a* and *b* plane are held together by hydrogen bonds. Figure 4 depicts the crystal axes.

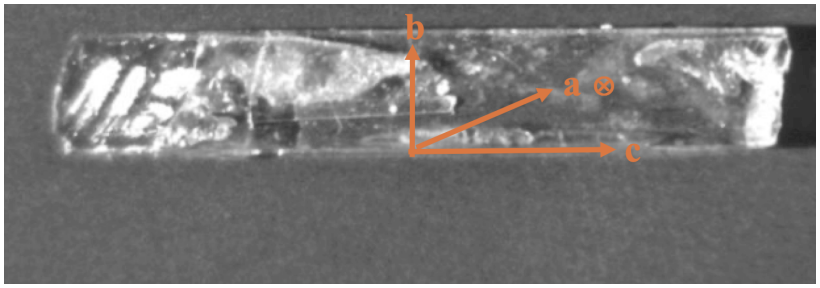

Fig. 4 Crystal axes are labeled on a PETN single crystal.

The sample mounts were originally made from aluminum, but due to manufacturing difficulties, 3D-printed designs were later preferred. A bridge-wire detonator was placed through the bottom of the mount up to the slot containing the PETN sample. Finally, a polycarbonate cover was placed above the slot to contain the PETN and also provide optical access for imaging. All components were fastened together using stainless steel screws and nuts. Figure 5 shows a sample mount and its components.

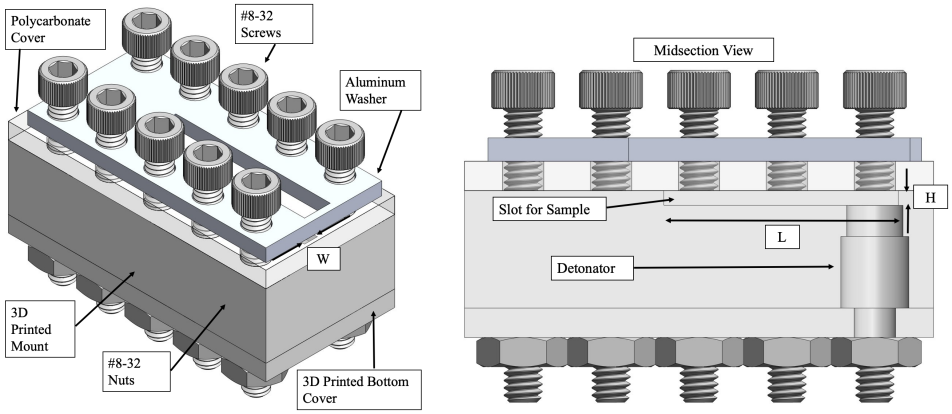

Fig. 5 The "loose-powder" sample mount and its cross-section are shown.

Four types of sample mounts were developed. The first, called the "loose-powder mount", involved the placement of 75-100mg of PETN powder without packing. Figure 5 shows this type of mount. Next, a "packed-powder mount" was made, which allowed for 50-75mg of PETN powder to be packed up to 70 TMD. It included an aluminum plate which constrained the sample through the side. This is shown in Fig. 6. Third was a "crystal mount" which had a slot large enough for a single crystal. It included a plastic cover that secured the detonator to the sample. Earlier versions of the design, which placed the detonator against the bottom of the crystal, or along the *a* and *b*-axis, are tested. This is shown in Fig. 7. Lastly, a combination of packed-powder and crystal was developed. The purpose of this was to impart more kinetic and thermal energy onto the crystal than possible with a static detonator. Figure 8 showcases this mount. Due to the parallel timeline of developing the mounts and running experiments, only the first three types of mounts are tested in this report.

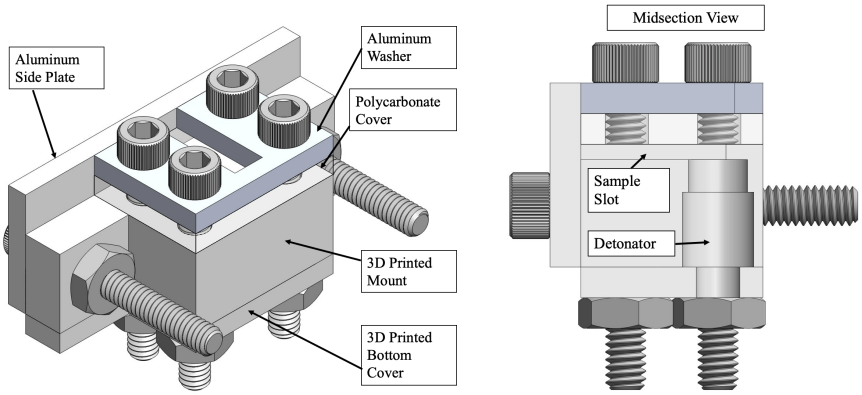

Fig. 6 The packed powder sample mount and its cross-section are shown.

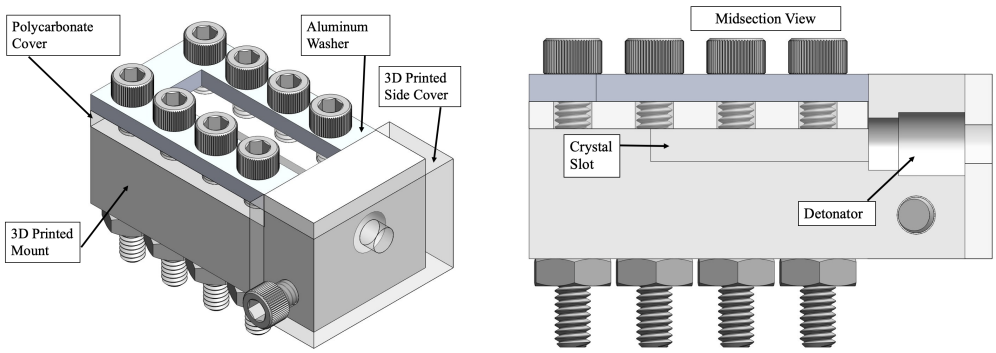

Fig. 7 The crystal sample mount and its cross-section are shown.

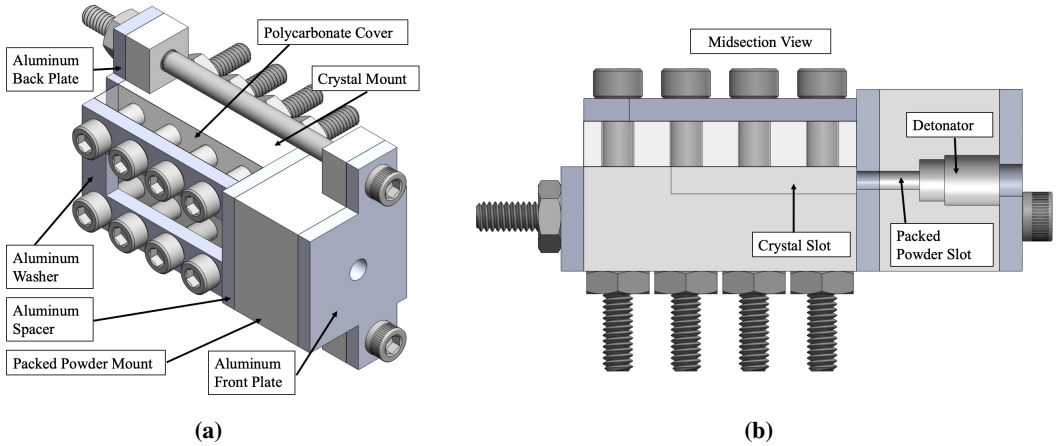

Fig. 8 The packed-powder and crystal combination sample mount and its cross-section are shown.

Sample mounts were assembled and then put inside the detonation box and secured to an optical table. The samples were placed approximately two inches away from the window frame to allow for the correct focus and magnification on the Shimadzu camera and lens. In every experiment, each sample was sequentially labeled with a letter D followed by the sample number. The setup can be seen in Fig. 9.

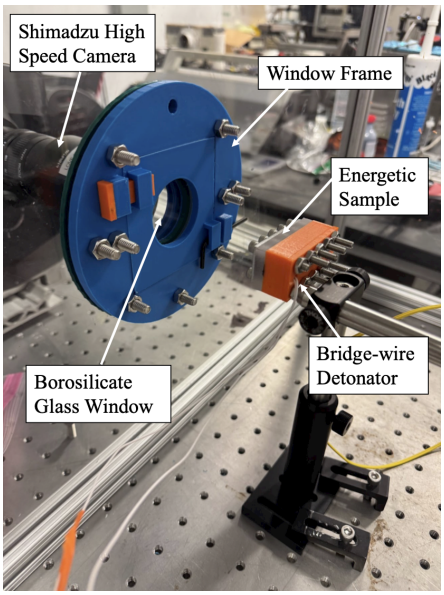

Fig. 9 The experimental setup of a sample mount is seen.

The camera was placed outside of the box, looking through the borosilicate glass window. In between the camera lens and the window was a Neutral Density (ND) filter and a protective glass frame to prevent any explosive material from damaging the lens. This is seen in Fig. 3a.

IV. Testing and Results

Initial testing began in August 2024 inside the prototype box and with older mount designs. After these experiments, the current versions of the sample mounts and the new detonation box were developed. The following results were from experiments conducted in October 2024, November 2024, and February 2025. Table 1 depicts the sample number and PETN type, along with the mass and estimated packing density. It can be noted that PETN crystals are considered to have 100% packing density; however, any voids or gaps during formation may reduce the true value.

Table 1 PETN Sample Data

Sample	PETN Mass (mg)	PETN Phase	Packing Density (%)	Particle Size (mm)	Detonator	Casing	LWH Slot Dimension (mm)
D04	100	Semi Packed Powder	≈ 40	0.2-0.4	BW	ALU	55.0 x 3.50 x 3.50
D08	50	Loose-Powder	18.8	0.2-0.4	BW	3DP	38.1 × 2.54 × 1.59
D09	396	Crystal	100	-	BW	3DP	22.2 × 6.35 × 3.97
D10	75	Loose-Powder	27.8	0.2-0.4	BW	3DP	38.1 × 2.54 × 1.59
D11	75	Loose-Powder	27.8	0.2-0.4	BW	3DP	38.1 × 2.54 × 1.59
D12	50	Packed-Powder	48.7	<0.2	BW	3DP	38.1 × 2.54 × 1.59

A. Detonation

The following images were taken by the Shimadzu camera of the detonation for each sample.

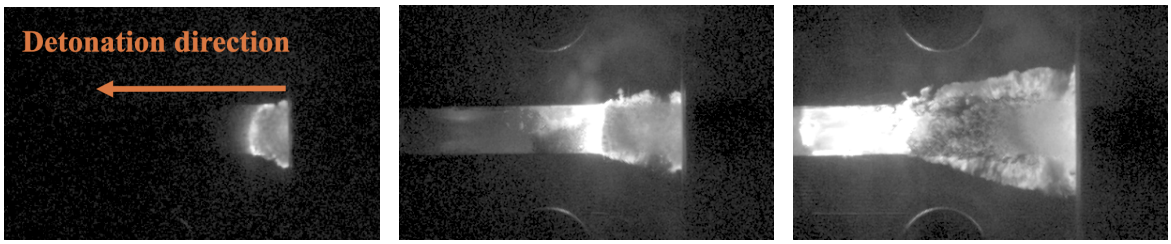

(a) (b) (c)

Fig. 10 The wave propagation of sample D04 is shown.

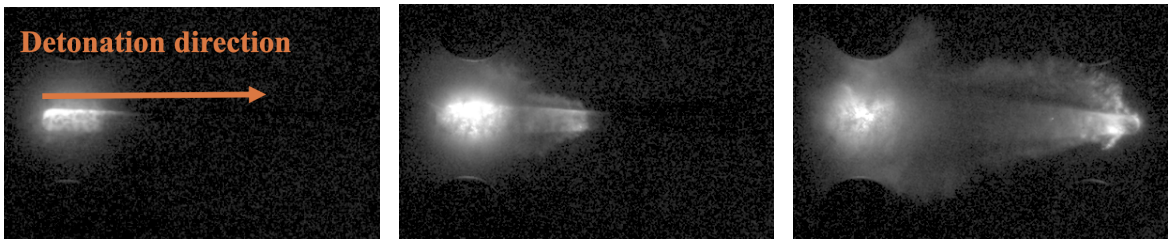

(a) (b) (c)

Fig. 11 The wave propagation of sample D08 is shown.

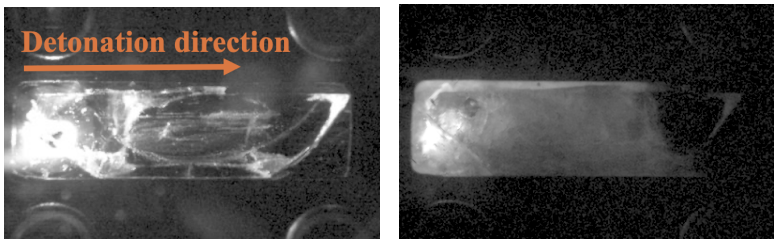

(a) (b)

Fig. 12 The detonation attempt of sample D09 is shown.

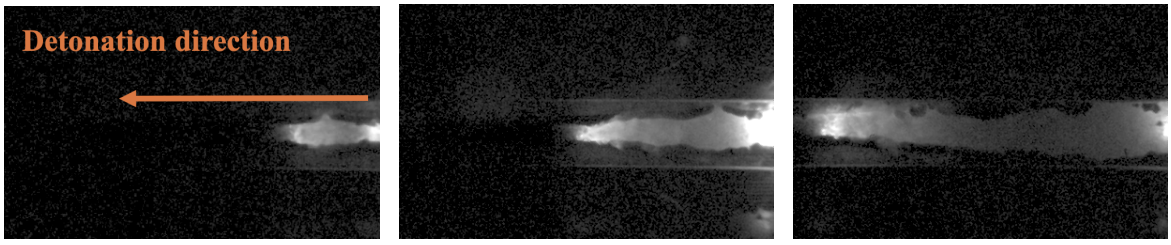

(a) (b) (c)

Fig. 13 The wave propagation of sample D10 is shown.

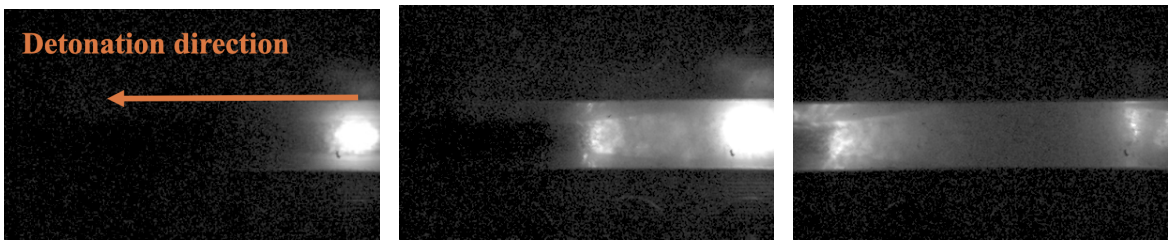

(a) (b) (c)

Fig. 14 The wave propagation of sample D11 is shown.

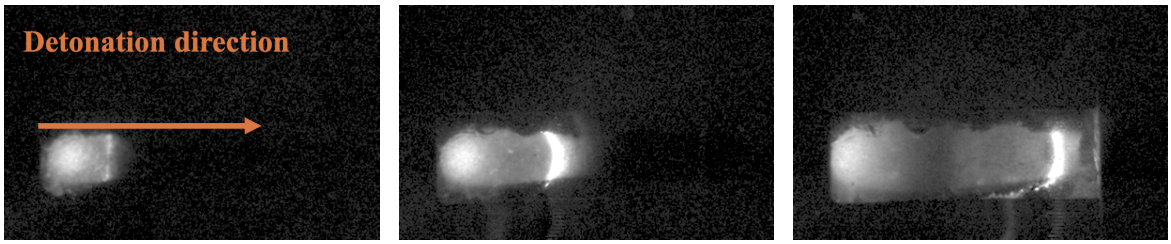

(a) (b) (c)

Fig. 15 The wave propagation of sample D12 is shown.

In sample D04, an initial planar propagation occurs followed by a complete particle ejection. This is shown by the bright spots in 10c. This particle ejection may have caused faults in velocity analysis and true performance.

In sample D08, it can be observed in Fig. 11c that powder mass escaped through a pressure leak between the polycarbonate cover and the mount. In order to contain the pressure better, the aluminum "washer" was later added above the polycarbonate panel (without obstructing the view of the sample). In samples D10 through D12, this addition is shown to increase deflagration velocity.

A key point to note in sample D12 is that an initial planar wave, seen in Fig. 15a, is visible, which then develops into a bowed out wave, seen in Fig. 15c. The bowing occurs due to boundary effects from the slot walls. These effects may transfer to and slow down the wave vertex, or the leading point on the curve. This may be minimized by widening the slot, which prevents boundary effects from reaching the vertex.

B. Velocimetry Analysis

The Shimadzu camera captured 256 frames of the detonation, which totals to 25.6 μs of recording time. Using MATLAB, splices of each image located at the center of the slot width were overlaid in order to create a distance vs. time chart. This is shown in Fig. 16. The slope of the visible line corresponded to the wave velocity, which was then assessed to determine the type of wave. Points of a certain brightness threshold were selected, and a line-of-best-fit was computed. The bright spots near the bottom of each image overlay correspond to light from the detonator, which appear as pulses on video and are visible for the duration of the recording.

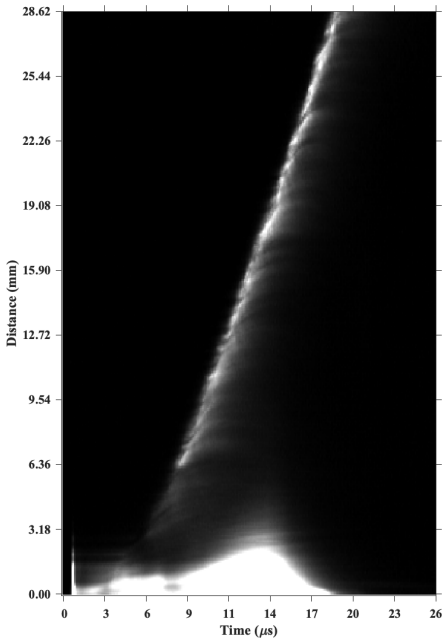

Fig. 16 A spliced image overlay of sample D10 is shown.

A temporal trend emerged in each of the PETN powder samples, which involved a delay after the initial ignition by the detonator, then a slower run-up of the powder which transitioned into a faster detonation wave. This phenomenon is known as the Deflagration to Detonation Transition (DDT). The type of wave is determined by the velocity in relation to the speed of sound in PETN, which is about 2000 m/s [6]. A deflagration is a subsonic wave and reaction zone in the energetic material, and a detonation occurs when a shock travels at or above sonic velocity and is followed by a reaction zone in the material.

For each sample, two lines of best fit for each powder-sample were computed, as a slower run-up was observed before the faster wave. This can be best observed in Fig. 17, which shows the image-splice overlay in sample D08.

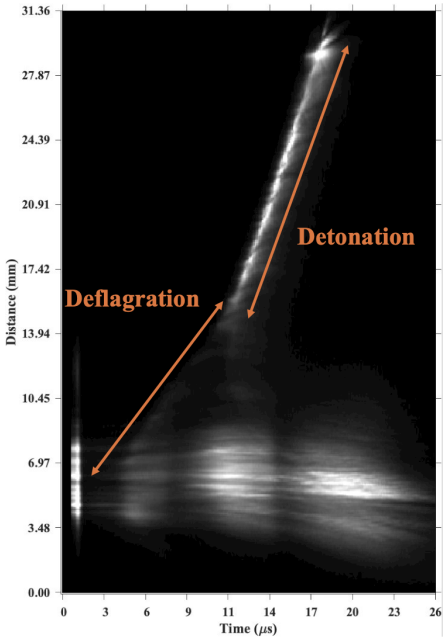

Fig. 17 The spliced image overlay of D08, along with the deflagration and detonation region, is shown.

Table 2 details the sample velocities. The detonation velocities were compared to the velocity at 100% TMD, which is 8350 m/s [7].

Table 2 Sample Velocities

Sample	Packing Density (%)	Deflagration Velocity (m/s)	Detonation Velocity (m/s)
D04	≈ 40	2066.9104	3325.6071
D08	18.7	1009.6826	2251.0023
D10	27.8	1449.0914	2162.5523
D11	27.8	1626.9099	2114.4298
D12	48.7	1215.7778	3589.2213

C. Results

From Table 2, it is seen that increasing packing density is observed to increase the detonation velocity and reduce time and distance before DDT. Deflagration velocity also seemed to change based on how tightly secured the sample mount covers were to the mount. As previously mentioned, D08 had mass escape through pressure leaks between the 3D printed mount and the polycarbonate cover. With the addition of the aluminum washer to D10 and onward, the deflagration velocity showed improvement.

Crystal detonation proved a challenge with the detonator mounted in the *a* and *b*-axis direction rather than the preferred *c*-axis. Sample D09 was tested twice to fully assess the performance of the crystal. On first fire, the detonator cracked the PETN crystal but did not result in a reaction. The second fire cracked the crystal slightly more but still did not result in a reaction.

Lastly, each powder detonation proved to completely destroy the sample mount. Tests conducted in October and November also showed that some shrapnel hit the borosilicate glass window and shattered it. In subsequent iterations, the window mount was improved to make replacement and cleanup of glass shards easier. However, in the February tests, the addition of the aluminum washer resulted in the energy concentrating onto the 3D-printed mount, which prevented any damage to the window.

V. Conclusion and Next Steps

The development of the novel sample mount proved to be reliable and well-suited for for imaging PETN detonations. Depicted in Section IV.A, a clear detonation wave in the samples were observed, along with the run-up to detonation. The containment of explosive pressure and increasing packing density corresponded with a faster and more uniform detonation wave that was easier to analyze. The more robust sample mount had a second benefit in protecting equipment such as the camera lens and borosilicate glass window. The design was also easily replaceable and manufacturing times decreased.

The velocimetry analysis yielded a key observation that increasing the packing density of PETN powder will lead to higher velocity and better performance. More tests at varying packing densities are needed to further develop a numerical correlation between these parameters. Future experiments are slated to increase the packing density to about 70%, along with modifying the slot dimensions in order to maximize uniformity.

More testing is necessary in order to prove the ability of PETN crystals to detonate with the updated sample mount design. From Sample D09, the crystal is able to initiate, though ignition in the *c*-axis direction may be necessary in order for it to properly detonate. Some other methods to detonate the crystal may include introducing surface voids to increase surface area, allow for hot-spot formation, and allow for easier avenues of propagation.

A future round of testing will include tracking particles in order to determine the behavior of the PETN before and after the detonation wave. This can be achievable using Digital Image Correlation (DIC), a method to characterize the bulk movement of a sample by tracking individual particles. These tracking particles will have to be on the order of 1 to 10 μm in diameter in order to visibly identify them alongside the PETN particles. A challenge with this includes the filtering of the initial light of the explosion, which is known to peak within the visible light and ultraviolet spectrum [8].

Lastly, increasing the camera magnification while imaging the sample will allow for the study of individual particle

reactions and initial behavior during ignition. In order to do this, the sample must be placed closer to the camera, which risks damaging the lens. The recent sample mount design may be able to solve this issue, as directing the energy of the explosion away from the borosilicate glass window proved its safety and effectiveness.

VI. Acknowledgments

This work was sponsored by the Air Force Office of Scientific Research (AFOSR) under grant/contract number FA9550-23-1-0534. The views and conclusions contained herein are those of the authors and should not be interpreted as necessarily representing the official policies or endorsements, either expressed or implied, of the Air Force Office of Scientific Research or the U.S. Government.

References

[1] Korepanov, V., Lisitsyn, V., Oleshko, V., and Tsypilev, V., "PETN detonation initiated by a high-power electron beam," *Technical Physics Letters*, Vol. 29, 2003, pp. 669–671.

[2] Coronel, S. A., and Kaneshige, M. J., "Response of PETN detonators to elevated temperatures," *Proceedings of the Combustion Institute*, Vol. 38, No. 3, 2021, pp. 4271–4279.

[3] Halfpenny, P., Roberts, K., and Sherwood, J., "Dislocations in energetic materials: I. the crystal growth and perfection of pentaerythritol tetranitrate (PETN)," *Journal of crystal growth*, Vol. 67, No. 2, 1984, pp. 202–212.

[4] Varış, S., "Molecular modelling of some explosives and propellants," Ph.D. thesis, Middle East Technical University (Turkey), 2013.

[5] Zheng, A. X., Knepper, R., Damm, D., and Mazumdar, Y. C., "Optical Digital Image Correlation for the Study of Thermal Cycling and Mechanical Fracture of Energetic Materials," *AIAA SCITECH 2024 Forum*, 2024, p. 1926.

[6] Schulze, P., Lopez-Pulliam, I., Heatwole, E., Feagin, T., and Parker, G., "The deflagration-to-detonation transition (DDT) in high density pentaerythritol tetranitrate (PETN)," *AIP conference proceedings*, Vol. 2272, AIP Publishing, 2020.

[7] Bastea, S., Glaesemann, K., and Fried, L., "Equation of state for high explosives detonation products with explicit polar and ionic species," Tech. rep., Lawrence Livermore National Lab.(LLNL), Livermore, CA (United States), 2006.

[8] Renlund, A. M., and Trott, W., "Spectra of visible emission from detonating PETN and PBX 9407," Tech. rep., Sandia National Lab.(SNL-NM), Albuquerque, NM (United States), 1984.